Spatial organization of a replicating bacterial chromosome

Idit Anna Berlatzky, Alex Rouvinski, and Sigal Ben-Yehuda*

Department of Molecular Biology, Institute of Medical Research, Faculty of Medicine, POB 12272, Hebrew University of Jerusalem, Jerusalem 91120, Israel

Edited by Richard M. Losick, Harvard University, Cambridge, MA, and approved July 31, 2008 (received for review June 14, 2008)

Emerging evidence indicates that the global organization of the bacterial chromosome is defined by its physical map. This architectural understanding has been gained mainly by observing the localization and dynamics of specific chromosomal loci. However, the spatial and temporal organization of the entire mass of newly synthesized DNA remains elusive. To visualize replicated DNA within living cells, we developed an experimental system in the bacterium *Bacillus subtilis* whereby fluorescently labeled nucleotides are incorporated into the chromosome as it is being replicated. Here, we present the first visualization of replication morphologies exhibited by the bacterial chromosome. At the start of replication, newly synthesized DNA is translocated via a helical structure from midcell toward the poles, where it accumulates. Next, additionally synthesized DNA forms a second, visually distinct helix that interweaves with the original one. In the final stage of replication, the space between the two helices is filled up with the very last synthesized DNA. This striking geometry provides insight into the three-dimensional conformation of the replicating chromosome.

Bacillus subtilis | bacterial cell biology | DNA replication | nucleoid | replisome

Faithful DNA replication and segregation are essential for all prokaryotic and eukaryotic cells to maintain their genomic integrity. The topological features of DNA, combined with its enormous length, raise the fundamental questions of how replication is organized spatially and what is the geometry of the replicating chromosome. These questions are even more crucial for bacteria, because they are capable of initiating a new round of DNA replication before the previous round has been completed, resulting in multifork replication (1). Moreover, bacteria lack a nucleus compartmentalizing their DNA; instead the bacterial DNA mass (nucleoid) occupies the majority of the cytoplasmic space. Nevertheless, the nucleoid appears as a well organized structure in which chromosome replication and partitioning are carried out with remarkable spatial and temporal regulation (2–9).

Like many bacteria, *Bacillus subtilis* has a single circular chromosome (≈4,200 kilobase pairs), where DNA replication is initiated from a single origin (*oriC*) and proceeds bidirectionally. Visualization of specific *B. subtilis* chromosomal loci has revealed that, in general, the *oriC* regions are duplicated at the cell center and then move toward opposite poles, whereas the unduplicated terminus region remains centrally located throughout the replication process (10–14). The replication machinery (replisome) is composed of two complexes, one for each replication fork, that tend to remain at midcell during chromosome duplication (15, 16). It has been proposed that unduplicated DNA is pulled into the replisome and newly synthesized DNA is extruded bidirectionally from the complex (4, 16).

The spatial and temporal organization of the replicating bacterial chromosome has been elucidated mainly by observing the localization and dynamics of specific chromosomal loci (2–9). As opposed to observing specific sequences, we developed an experimental model system for visualizing the overall geometry of the newly synthesized DNA in living *B. subtilis* cells. Our data uncover previously uncharacterized morphologies of the replicating chromosome and provide the basis for our model describing the spatial organization of the nucleoid during replication.

Results

Incorporating Fluorescent Nucleotides into the Chromosome of Living *B. subtilis* Cells. To visualize the overall geometry of replicated DNA in living *B. subtilis* cells, we attempted to develop an experimental system by which we could observe the global mass of the newly synthesized DNA as it is being replicated. Our strategy was based on incorporating fluorescently labeled nucleotides into the chromosome of cells undergoing replication and, thus, to directly visualize the localization patterns of newly duplicated DNA by using fluorescence microscopy. Because negatively charged deoxynucleotide triphosphates (dNTPs) do not normally traverse the plasma membrane, we searched for a method that would enable us to efficiently deliver small molecules into living cells. Thus, we treated *B. subtilis* cells with various substances and identified Pluronic F-68 as an agent that enhances the uptake of small molecules (17). Importantly, we established that Pluronic F-68 has no effect on the growth, morphology, or viability of cells [see supporting information (SI) *Text* and Fig. S1]. In addition to optimizing delivery of fluorescent nucleotides, we had to devise a way to ensure their effective incorporation. Because fluorescent nucleotides are unnatural substrates for DNA polymerase, we reasoned that they would be incorporated more efficiently when natural nucleotides are deprived. Therefore, we attempted to visualize replication patterns in cells growing under minimal conditions. Moreover, the use of minimal medium circumvents the complication of observing multifork replication in a single cell (16, 18). Indeed, cells grown under these conditions underwent only one round of replication per cell division, as indicated by the presence of only two copies of origin regions in most cells (Fig. S2*A*) (10–14, 19).

To visualize the newly synthesized DNA in living cells, wild-type *B. subtilis* cells (PY79) were grown in minimal medium in the presence of Pluronic F-68, and fluorescent nucleotides were added to the culture during the early logarithmic phase. The uptake and incorporation of the labeled nucleotides were then examined by using fluorescence microscopy. Although no significant fluorescence was detected at early times, after a few generations, we observed a clear fluorescent signal within the majority of the cells (see *Materials and Methods*). As shown in Fig. 1*A*, the fluorescent nucleotides frequently assembled into elongated structures and were not simply diffused throughout the cytoplasmic space. Further experiments (*SI Text* and Figs. S3 and S4) confirmed that, indeed, the unnatural nucleotides are

Author contributions: I.A.B., A.R., and S.B.-Y. designed research; I.A.B., A.R., and S.B.-Y. performed research; I.A.B. and A.R. contributed new reagents/analytic tools; I.A.B., A.R., and S.B.-Y. analyzed data; and I.A.B., A.R., and S.B.-Y. wrote the paper.

The authors declare no conflict of interest.

This article is a PNAS Direct Submission.

*To whom correspondence should be addressed. E-mail: sigalb@ekmd.huji.ac.il.

This article contains supporting information online at www.pnas.org/cgi/content/full/0804982105/DCSupplemental.

www.pnas.org/cgi/doi/10.1073/pnas.0804982105

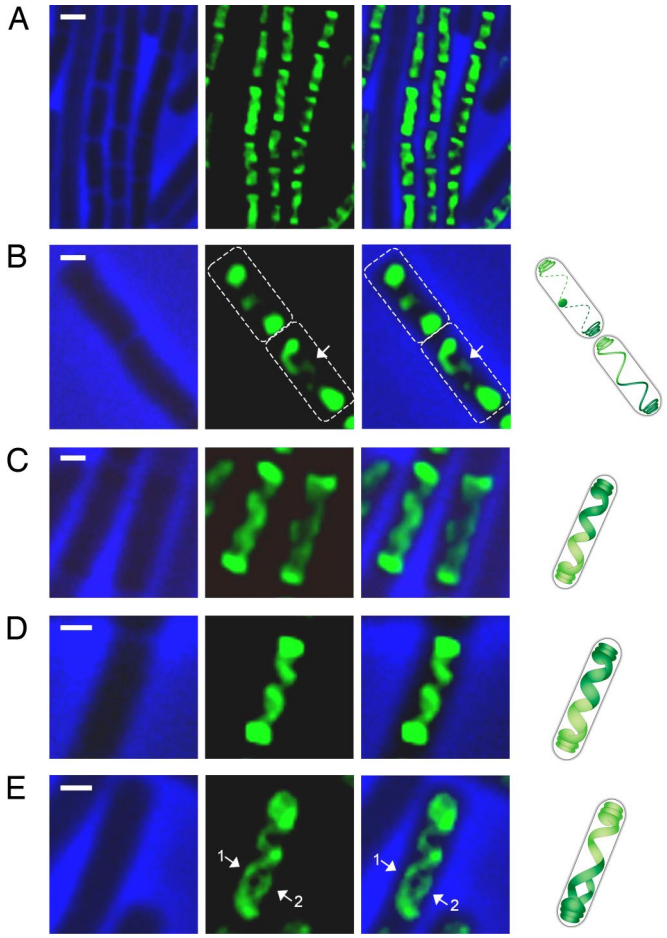

Fig. 1. Visualizing localization patterns of newly replicated DNA. (*A*) A growing culture of *B. subtilis* cells (PY79) was treated with fluorescent nucleotides and photographed 2 h after the start of detectable incorporation (*Materials and Methods* and *SI Text*). Cells were observed with phase-contrast microscopy (blue, *Left*), and the localization of the incorporated nucleotides was observed by fluorescence microscopy (green, *Center*). (*Right*) An overlay of the signals from fluorescent nucleotides and phase contrast. Note that the nucleotides were not incorporated into the DNA of all of the cells in the field. (Scale bar: 1 μm.) (*B–E*) A growing culture of *B. subtilis* cells (PY79) was treated with fluorescent nucleotides (*Materials and Methods* and *SI Text*) and photographed at 30-min intervals after the start of detectable incorporation. Shown are typical localization patterns of the fluorescent nucleotides (green) observed from early until late stages of replication (*B* to *E*, respectively). Cells are shown by phase-contrast microscopy (blue). (*Right*) Interpretive cartoons in which the two copies of the newly synthesized DNA are represented by different tones of green. The dashed line in *B* illustrates cell borders, and the arrow highlights the filament connecting the polar foci. Arrows in *E* indicate the position of the two helices: initial helix (1) and sequential helix (2). (Scale bars: 0.5 μm.)

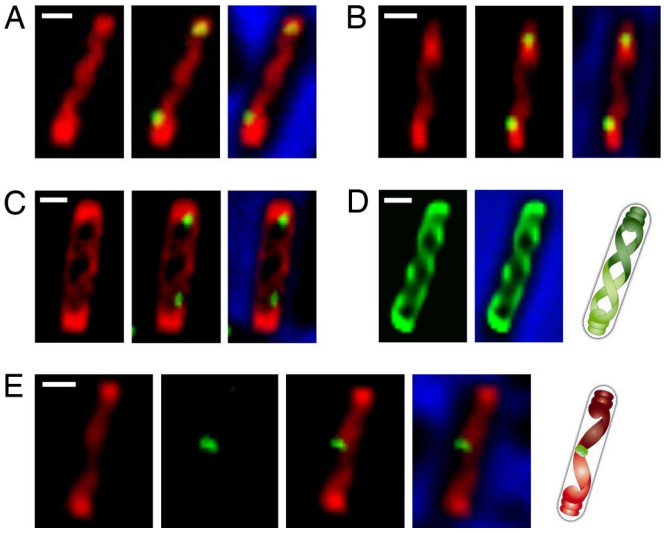

Fig. 2. Temporal and spatial organization of the replicating chromosome. (*A–C*) Visualization of the origin regions with the newly replicated DNA. Fluorescent nucleotides were added to a growing culture of *B. subtilis* cells (SB294), producing a GFP fusion to Spo0J that binds to the origin regions; cells were photographed at 30-min intervals after the start of detectable incorporation (*Materials and Methods* and *SI Text*). The localization of Spo0J-GFP was observed with respect to the different stages of replication. Shown are fluorescence from the incorporated nucleotides (red), fluorescence from Spo0J-GFP (green), and bacterial cells by phase contrast (blue). (*D*) Deconvolution microscopy revealing the interweaving helices formed by the newly replicated DNA. A growing culture of *B. subtilis* cells (PY79) was treated with fluorescent nucleotides, and optical sections were collected 2 h after the start of detectable incorporation (*Materials and Methods* and *SI Text*). Shown is deconvolution microscopy of the fluorescent signal from a typical cell revealing the three-dimensional structure of the two interweaving helices. The deconvolved image of the fluorescent signal is shown in green, and the cell outline is shown by phase contrast (blue). The image on the right shows an interpretive cartoon in which the two copies of the newly synthesized DNA are represented by different tones of green. (*E*) Visualization of DNA polymerase with the newly replicated DNA. Fluorescent nucleotides were added to a growing culture of *B. subtilis* cells (IB66), producing a GFP fusion to the τ DNA polymerase subunit (*Materials and Methods* and *SI Text*). Fluorescence from the incorporated nucleotides is shown in red, and fluorescence from GFP is shown in green. Also shown are overlay images of signals from fluorescent nucleotides and GFP with or without phase contrast (blue). The image on the right shows an interpretive cartoon in which the two copies of the newly synthesized DNA are represented by different tones of red, and the replisome is labeled in green. (Scale bars: 0.5 μm.)

efficiently incorporated into the replicating chromosome of *B. subtilis*, and these labeled nucleotides specifically signify the localization pattern of newly replicated DNA.

Visualizing the Dynamics of the Replicating Chromosome. We next carried out time-course experiments to explore the dynamics of the replicating chromosome. At early times after the start of detectable incorporation, the newly synthesized DNA accumulated mostly in large foci located close to both cell poles. Often, we were able to see an additional signal located at midcell that sometimes seemed to be part of a continuous filament connecting the two polar foci (Fig. 1*B*). The fluorescence observed in cells at later stages of replication revealed the filament structure to be helical, extending lengthwise across the cell (Fig. 1*C*); this structure became more pronounced as replication proceeded (Fig. 1*D*). In general, this helix had two turns; however, the turn number sometimes varied with cell length. Interestingly, fluorescence at the poles occasionally appeared as if it represented condensed helices and not simply foci. However, these structures were difficult to resolve because of their intense fluorescence. To visualize the localization of the origin region concomitantly with the helical structure formed by the newly synthesized DNA, we repeated the experiment using a strain harboring a GFP fusion to Spo0J (SB294), a protein that binds near the origin (12, 14, 20–22). GFP fluorescence was localized predominantly to both tips of the helical filament (Fig. 2*A*). Occasionally, when the fluorescent signal from the nucleotides was particularly strong near the poles, the localization of the origins seemed slightly closer to the cell center, as if they were pushed by the newly synthesized sequences accumulating at the poles (Fig. 2*B*).

Taken together, our results suggest that after replicating at midcell, the duplicated sequences are delivered to opposite regions close to the cell poles where they accumulate. The

translocation of the DNA from midcell toward the poles occurs via the formation of a helical filament that extends lengthwise across the cell. This seemingly continuous filament is composed of the two newly synthesized copies of the replicating chromosome, with each half of the filament corresponding to one of the two copies. Conceivably, the sequences delivered through the helical filament are packaged into a condensed coil at each pole. The thickening of the helical structure as replication proceeds may be due to a parallel bundling of additional replicated sequences onto the helix that need to be evacuated from midcell and translocated to the poles.

An important feature of our model is that DNA polymerase should be localized to the middle of the helix formed by the replicated sequences. By using a strain harboring a functional fusion of the Tau subunit to GFP (16), we observed that most cells exhibited one or two closely positioned foci of DNA polymerase localized predominantly at the cell center (Fig. S2*B*) consistent with previous reports (15, 16). Subsequently, when the Tau-GFP-producing cells were treated with red fluorescent nucleotides, the green fluorescence foci were chiefly detected at the center of the helix as predicted (Fig. 2*E*).

Further investigation of the sequential architectural patterns of the newly synthesized DNA indicated that at later times of replication a second helical structure was formed, spanning the length of the cell resembling the original one (Fig. 1*E*). To elucidate the three-dimensional nature of the structure formed by the two helices, stacks of optical sections were collected, and a deconvolution program was used. Fig. 2*D* shows three-dimensional deconvolution of a representative cell in which two clear replicated helices extending lengthwise across the cell were monitored. Often, we observed a clear void between the two filaments, implying that they do not occupy the entire inner space of the cell. However, in some cases, when fluorescence from the two helices was intense, they seemed embedded within each other. Superimposing the origins onto the two-helical structure revealed that they maintain their localization in the vicinity of the poles (Fig. 2*C*).

Differentiating Early from Late Replicated DNA. To obtain a better time resolution, we designed a two-color replication assay that enables differentiation of early from late replicated DNA. Wild-type cells were incubated initially with red fluorescent nucleotides. After incorporation began, the unincorporated red nucleotides were washed away, and a new pulse of green fluorescent nucleotides was added to the medium. In cells where both types of nucleotides were incorporated into the DNA, we were frequently able to see the typical initial helix formed in red and the second helical structure formed in green, implying that, indeed, the construction of the helices is sequential (Fig. 3*A*). To define the chromosomal architecture during final stages of replication, we searched for cells where red fluorescence was present in both helices and observed the pattern of the subsequently incorporated green nucleotides (Fig. 3*B*). Because the green fluorescence clearly occupied the spatial gap within the red helices, we concluded that the very last replicated sequences fill in the space between the two interweaving helical filaments.

Thus, in extension of our model, we infer that when a certain amount of replicated DNA has been accumulated at the poles, additionally synthesized sequences create a second helix that is interwoven with the original one. Similar to the first helix, this subsequent filament is composed of sequences from both chromosomes but appears as a continuous helix extending across the cell length. Initially, the helices are separated in space, creating a void in between them, probably where the unreplicated DNA is present. However, this gap is finally sealed by the most recently synthesized DNA. This complex structure demonstrates that late replicated sequences can lie in proximity to early replicated sequences.

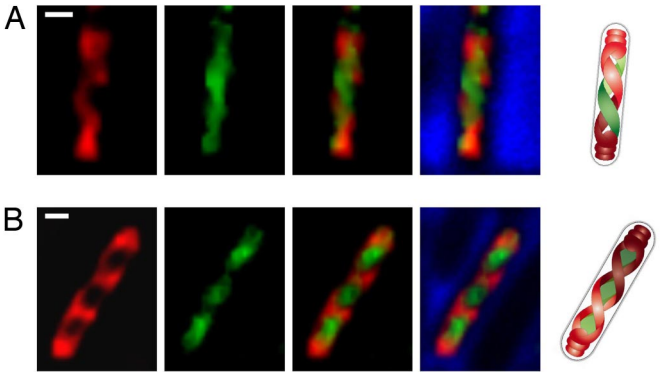

Fig. 3. Differentiating early from late replicated DNA. (*A* and *B*) Red fluorescent nucleotides were added to a growing culture of *B. subtilis* cells (PY79). One hour after incorporation was visible, the unincorporated red nucleotides were washed away, and green fluorescent nucleotides were added sequentially (*Materials and Methods* and *SI Text*). Shown are typical localization patterns of incorporated fluorescent nucleotides (red and green) observed when both nucleotides were incorporated into the DNA of the same cell. Also shown are overlay images of red and green signals from fluorescent nucleotides with or without phase contrast (blue). The images on the right show interpretive cartoons in which the two copies of early replicated DNA are represented by different tones of red, and the two copies of late replicated DNA are represented by different tones of green. (Scale bars: 0.5 μm.)

Visualizing the Chromosome Structure During Replication and Segregation in Living Cells. Our direct observations of replication patterns imply that the replicating chromosome must acquire a special helical structure that holds together the two newly formed chromosomes. If correct, these structures should also be seen when bacterial cells are treated with a standard fluorescent DNA dye such as 4′,6-diamidino-2-phenylindole (DAPI). Unlike the fluorescent nucleotides that exclusively mark newly synthesized DNA, DAPI stains the entire chromosomal mass. Nevertheless, despite this difference, helical shapes of the chromosome extending along the cells were frequently detected in a field of growing cells (Fig. 4*A*). As an alternative approach to stain DNA, we exploited a strain (MF60) that harbors a functional fusion of the β' subunit of RNA polymerase to GFP (*rpoC-gfp*). RNA polymerase binds the chromosome; therefore, this GFP fusion decorates the entire nucleoid mass. Similar to DAPI staining, helical patterns were readily detected in a population of growing MF60 cells (Fig. 4*B*). To test our hypothesis that these structures represent the replicating form of the chromosome, we carried out time-lapse microscopy to follow the nucleoid dynamics in individual MF60 cells during the cell cycle. While examining many individual cells, we observed very reproducible nucleoid patterns (Fig. 4*C* and Movie S1 and Movie S2). Notably, in preparation for partitioning, the two daughter chromosomes were condensed into a bilobed conformation (Fig. 4*C*1), which subsequently segregated into two separable chromosomes that appeared condensed (Fig. 4*C*2). However, soon after segregation and at a time that appeared to coincide with replication, the chromosome adopted a looser form that occupied a larger cell volume (Fig. 4*C*3). This chromosomal structure, which sometimes seemed helical, became elongated with time and was visible throughout much of the cell cycle. During that period, the nucleoid appeared as one integrative unit with no clear distinction between the two newly formed chromosomes. These results are consistent with a model in which, during replication, the nucleoid adopts a special replicating helical structure that contains the two newly formed chromosomes and is resolved when replication terminates.

Discussion

In the present study, we succeeded in visualizing the three-dimensional conformation of the replicating chromosome by

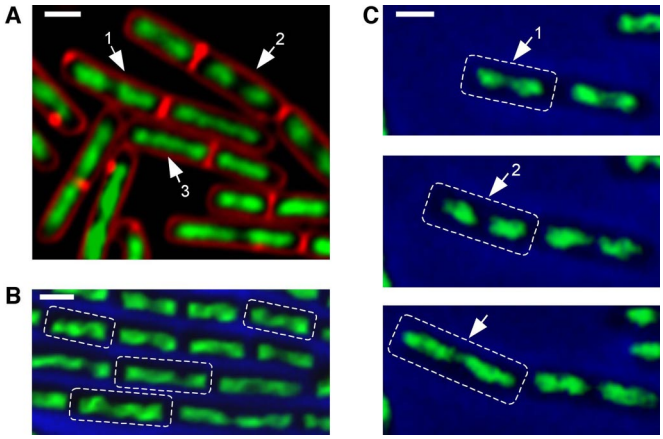

Fig. 4. Visualizing the chromosome structure during replication and segregation in living cells. (*A*) A typical field of growing *B. subtilis* cells (PY79) stained with DAPI (green) and FM4–64 membrane stain (red). The arrows highlight different typical morphologies of the nucleoid observed with DAPI staining: (1) bilobed nucleoid where the chromosomes are close to segregation, (2) fully segregated chromosomes, and (3) nucleoid forming a helical structure. (*B*) A typical field of growing *B. subtilis* cells (MF60) producing a GFP fusion to a RNA polymerase subunit (*rpoC-gfp*). Shown is an overlay image of signals from RpoC-GFP (green) and phase contrast (blue). The dashed lines highlights cells in which morphologies of the nucleoid resemble helical structures. (*C*) Time-lapse microscopy of MF60 (*rpoC-gfp*) cells. Cells were grown in minimal medium at 30°C. Shown are overlays of signals from RpoC-GFP (green) with phase-contrast images (blue) at 20-min intervals. Cell borders are indicated by the dashed lines, and the arrows highlight the different morphologies of the nucleoid as indicated in *A*. See corresponding Movie S1. (Scale bars: 1 μm.)

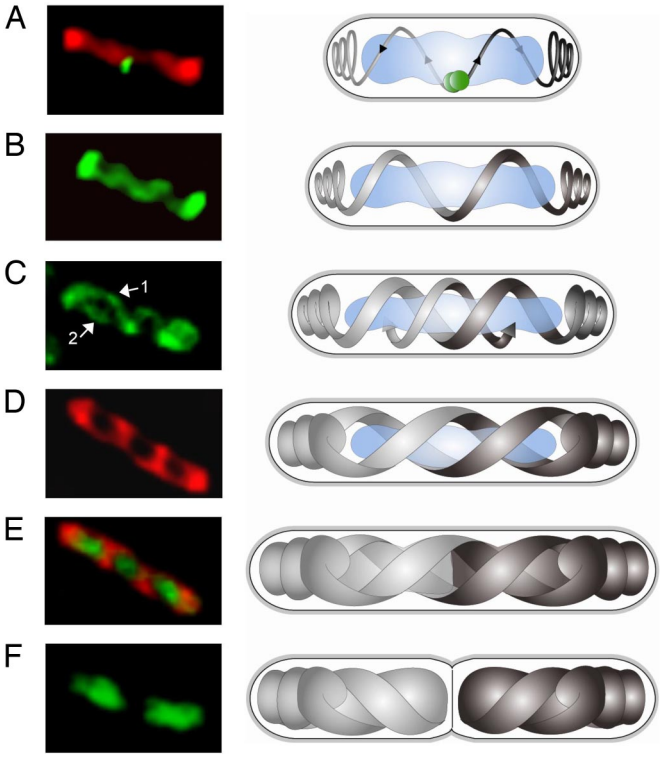

Fig. 5. A model for the geometry of the replicating chromosome in bacteria. (*Right*) Cartoons demonstrating our model for the geometry of the replicating chromosome. The two copies of the newly synthesized chromosomes are represented by the different tones of gray, the unreplicated chromosome is shown in light blue, and the replisome is shown in green. Arrowheads in *A* indicate the direction in which DNA is translocated after being replicated at midcell. (*Left*) The actual images of the corresponding stages illustrated by the cartoon model: Fig. 2*E* (*A*), Fig. 1*C* (*B*), Fig. 1*E* (*C*), Fig. 3*B* (*D*), Fig. 3*B* (*E*), and Fig. 4*C* (*F*).

incorporating fluorescent nucleotides into living *B. subtilis* cells. Importantly, our method seems to reveal the veritable pattern of replication, as shown by the following observations: First, DNA-binding proteins such as Spo0J and RpoC were able to recognize the modified DNA, as indicated by their proper localization. Second, several labeled nucleotides, coupled to various fluorophores used in this study exhibited similar localization patterns, suggesting that the type of modification has no effect on the spatial organization of the chromosome. Finally, replicating helical structures observed by incorporating the fluorescent nucleotides were also monitored by using standard DNA labeling methods, such as DAPI, which highlight the entire DNA mass. Based on our observations, we propose the following model, which may apply to other bacterial species (Fig. 5). At the onset of replication, the chromosome adopts an open conformation, enabling replication to initiate. The DNA is replicated by the replisome located at midcell, and the two newly synthesized copies are translocated via a helical structure to the opposite poles, accumulating there in a condensed coiled structure. The helical filament extends lengthwise across the cell, encircling the unreplicated DNA. Each half of the filament is generated by one of the two copies of the newly synthesized chromosomes (Fig. 5*A*). As replication proceeds, additional newly duplicated sequences are bundled together, forming a thicker helix through which they are translocated toward the poles (Fig. 5*B* and Fig. S5). When a sufficient mass of new DNA has been duplicated, the most recently synthesized sequences then initiate an alternative path, a second helix. The formation of the second helix may be due to the necessity for additional duplicated sequences to be delivered toward the poles, and/or it may be driven by the liberation of space previously occupied by the old diminishing chromosome. Similarly to the first one, the second helix progresses from midcell toward the poles (Fig. 5*C*). These two distinct interweaving helical filaments encase the residual unreplicated DNA (Fig. 5*D*). Because early replicated DNA occupies the regions near both poles, late replicated DNA is maintained as part of the helices, filling the space across the long axis of the cell. Finally, as the residual unreplicated DNA diminishes, the very last synthesized DNA fills the space between the two helices (Fig. 5*E*). This DNA may occupy the space between the helices by coalescing into the helices, thickening them or, alternatively, by simply piling the new sequences into the DNA-free space. When replication terminates, the newly replicated chromosomes are resolved, undergo condensation, and segregate into daughter cells (Fig. 5*F*).

Helical shapes have been shown to mediate various cellular processes in bacteria such as cell elongation and division. Additionally, several bacterial proteins form helical filaments that facilitate their dynamic cellular localization (7, 23–26). Here, we demonstrated that this abundant structure also directs the nucleoid morphology and may allow the replicated sequences to relocate from one cellular position to another. Furthermore, our model provides a spatial solution for the organization of replicated DNA relative to unreplicated DNA in a confined space. According to our model, the replicated and unreplicated regions are separable in space. The unreplicated DNA localizes to the inner part of the nucleoid mass, whereas the newly synthesized DNA encircles the unreplicated chromosome. This spatial separation may allow deferential management needed for unreplicated and postreplicated DNA. In the future, it will be of interest to employ our approach to resolve the even more complex structure of a chromosome undergoing multifork replication.

Our results support the notion that the bacterial nucleoid is organized into a highly ordered structure and that individual chromosomal loci localize to specific subcellular locations during bacterial DNA replication (2–9). However, our analyses imply that, at least for *B. subtilis*, the spatial localization of chromosomal loci does not simply correlate with their linear order on the physical map of the chromosome as proposed previously for other bacteria (7, 8). According to our two-color replication assay (Fig. 3), it seems that during late replication stages, the chromosome assumes a complex three-dimensional architecture in which late replicated sequences are placed in close proximity to early replicated ones. Gathering genes from distant chromosomal regions, to a similar subcellular localization, may mediate their actual biological function. Thus, it is possible that genes from similar functional groups, located at distant linear positions, associate spatially to coordinate their regulation. Moreover, it is possible that this regulation is dynamic, allowing different combinations of genes to associate spatially under various physiological conditions. We anticipate that spatial regulation of genes will prove to be a feature of many living organisms.

Materials and Methods

Strains and General Methods. *B. subtilis* strains were derivatives of the wild-type strain PY79 (27) and are listed in Table S1. All general methods were carried out as described (28).

Incorporation of the Fluorescent Nucleotides into the DNA of Living Cells. For all of the experiments performed, cells were grown in S7 minimal medium containing glucose (2%) as described (29), except that glutamic acid was added at a final concentration of 200 mM. Cells were grown overnight at 23°C in the presence of 0.3% Pluronic F-68 to early logarithmic phase (O.D. = 0.15). Next, Pluronic F-68 concentration was elevated to 3% concomitantly with the addition of fluorescently labeled nucleotides (for additional information see *SI Text*) at a final concentration of 3 μM. Cells were shaken at 37°C in the dark. At various times, samples (0.05 ml) were collected, washed in PBS to remove excess fluorescent nucleotides, briefly centrifuged, and visualized by fluorescence microscopy.

The time of nucleotide incorporation was somewhat variable between the experiments; therefore, in each experiment, samples were taken every 30 min for microscopic examination, and t0 was defined as the time that we first observed a fluorescent signal within the cells. In all of the described experiments, incorporation started a few generations after the addition of the fluorescent nucleotides during late logarithmic phase (Fig. S1*B*). We believe that this delay in incorporation depends on the physiological condition of the cells and not on the fluorescent nucleotides or the permeabilization period, because we found that adding the nucleotides shortly before late logarithmic phase (3 h after the increase in Pluronic F-68 concentration) resulted in an efficient and rapid incorporation (data not shown). It is possible that at this stage, the nutrients become limited, allowing the incorporation of unnatural nucleotides into the DNA.

General Fluorescence Microscopy Methods. Fluorescence microscopy was carried out as described (30). For observing replication patterns, slides were prepared by placing a silicone isolator (Sigma) on a glass slide and filling the wells with S7 medium containing 1.5% agarose. For time-lapse microscopy, MF60 cells were grown in S7 minimal medium to midlogarithmic phase, and samples of 0.1 ml were concentrated, applied to agarose pads, incubated at 30°C, and photographed at different time intervals. For all experiments, cells were visualized and photographed by using an Axioplan2 microscope (Zeiss) equipped with a CoolSnap HQ camera (Photometrics, Roper Scientific) or an AxioObserver Z1 microscope (Zeiss) equipped with a CoolSnap HQII camera (Photometrics, Roper Scientific). System control and image processing were performed by using MetaMorph software (Molecular Devices).

Deconvolution Microscopy. Samples of cells grown in the presence of Pluronic F-68 and fluorescently labeled nucleotides were concentrated, applied to agarose pads, and then subjected to deconvolution microscopy. Optical sections (20–50) of the signal from the fluorescent nucleotides were collected at a spacing of 0.1 μm. The images were deconvolved through 100 iterations by using the AutoQuant Widefield 3D deconvolution software (MetaMorph software; Molecular Devices).

ACKNOWLEDGMENTS. We thank M. Fujita (University of Houston, Houston) A. Grossman (Massachusetts Institute of Technology, Cambridge, MA), and A. Taraboulos (Hebrew University) for strains and reagents and R. Losick (Harvard University, Cambridge, MA), D. Kearns (Indiana University, Bloomington, IN), and members of the S.B.-Y. laboratory for valuable comments on the manuscript. This work was supported by Human Frontier Science Program Young Investigator Award RGY78/2007 and by United States–Israel Binational Foundation Grant 2005235 (to S.B.-Y.).

1. Cooper S, Helmstetter CE (1968) Chromosome replication and the division cycle of *Escherichia coli* B/r. *J Mol Biol* 31:519–540.
2. Hazan R, Ben-Yehuda S (2006) Resolving chromosome segregation in bacteria. *J Mol Microbiol Biotechnol* 11:126–139.
3. Hiraga S (2000) Dynamic localization of bacterial and plasmid chromosomes. *Annu Rev Genet* 34:21–59.
4. Lemon KP, Grossman AD (2001) The extrusion-capture model for chromosome partitioning in bacteria. *Genes Dev* 15:2031–2041.
5. Nielsen HJ, Li Y, Youngren B, Hansen FG, Austin S (2006) Progressive segregation of the *Escherichia coli* chromosome. *Mol Microbiol* 61:383–393.
6. Sherratt DJ (2003) Bacterial chromosome dynamics. *Science* 301:780–785.
7. Thanbichler M, Shapiro L (2008) Getting organized—How bacterial cells move proteins and DNA. *Nat Rev Microbiol* 6:28–40.
8. Viollier PH, *et al.* (2004) Rapid and sequential movement of individual chromosomal loci to specific subcellular locations during bacterial DNA replication. *Proc Natl Acad Sci USA* 101:9257–9262.
9. Wang X, Possoz C, Sherratt DJ (2005) Dancing around the divisome: Asymmetric chromosome segregation in *Escherichia coli*. *Genes Dev* 19:2367–2377.
10. Lee PS, Lin DC, Moriya S, Grossman AD (2003) Effects of the chromosome partitioning protein Spo0J (ParB) on *oriC* positioning and replication initiation in *Bacillus subtilis*. *J Bacteriol* 185:1326–1337.
11. Lewis PJ, Errington J (1997) Direct evidence for active segregation of *oriC* regions of the *Bacillus subtilis* chromosome and co-localization with the SpoOJ partitioning protein. *Mol Microbiol* 25:945–954.
12. Lin DC, Levin PA, Grossman AD (1997) Bipolar localization of a chromosome partition protein in *Bacillus subtilis*. *Proc Natl Acad Sci USA* 94:4721–4726.
13. Teleman AA, Graumann PL, Lin DC, Grossman AD, Losick R (1998) Chromosome arrangement within a bacterium. *Curr Biol* 8:1102–1109.
14. Webb CD, *et al.* (1997) Bipolar localization of the replication origin regions of chromosomes in vegetative and sporulating cells of *B. subtilis*. *Cell* 88:667–674.
15. Berkmen MB, Grossman AD (2006) Spatial and temporal organization of the *Bacillus subtilis* replication cycle. *Mol Microbiol* 62:57–71.
16. Lemon KP, Grossman AD (1998) Localization of bacterial DNA polymerase: Evidence for a factory model of replication. *Science* 282:1516–1519.
17. Murhammer DW, Goochee CF (1988) Scaleup of insect cell cultures: Protective effects of Pluronic F-68. *Biotechnology* 6:1411–1420D.
18. Nielsen HJ, Youngren B, Hansen FG, Austin S (2007) Dynamics of *Escherichia coli* chromosome segregation during multifork replication. *J Bacteriol* 189:8660–8666.
19. Sharpe ME, Errington J (1998) A fixed distance for separation of newly replicated copies of *oriC* in *Bacillus subtilis*: Implications for co-ordination of chromosome segregation and cell division. *Mol Microbiol* 28:981–990.
20. Glaser P, *et al.* (1997) Dynamic, mitotic-like behavior of a bacterial protein required for accurate chromosome partitioning. *Genes Dev* 11:1160–1168.
21. Lin DC, Grossman AD (1998) Identification and characterization of a bacterial chromosome partitioning site. *Cell* 92:675–685.
22. Murray H, Ferreira H, Errington J (2006) The bacterial chromosome segregation protein Spo0J spreads along DNA from *parS* nucleation sites. *Mol Microbiol* 61:1352–1361.
23. Ben-Yehuda S, Losick R (2002) Asymmetric cell division in *B. subtilis* involves a spiral-like intermediate of the cytokinetic protein FtsZ. *Cell* 109:257–266.
24. Cabeen MT, Jacobs-Wagner C (2007) Skin and bones: The bacterial cytoskeleton, cell wall, and cell morphogenesis. *J Cell Biol* 179:381–387.
25. Graumann PL (2007) Cytoskeletal elements in bacteria. *Annu Rev Microbiol* 61:589–618.
26. Jones LJ, Carballido-Lopez R, Errington J (2001) Control of cell shape in bacteria: Helical, actin-like filaments in *Bacillus subtilis*. *Cell* 104:913–922.
27. Youngman P, Perkins JB, Losick R (1984) Construction of a cloning site near one end of Tn917 into which foreign DNA may be inserted without affecting transposition in *Bacillus subtilis* or expression of the transposon-borne *erm* gene. *Plasmid* 12:1–9.
28. Harwood CR, Cutting SM (1990) *Molecular Biological Methods for Bacillus* (Wiley, New York).
29. Vasantha N, Freese E (1980) Enzyme changes during *Bacillus subtilis* sporulation caused by deprivation of guanine nucleotides. *J Bacteriol* 144:1119–1125.
30. Bejerano-Sagie M, *et al.* (2006) A checkpoint protein that scans the chromosome for damage at the start of sporulation in *Bacillus subtilis*. *Cell* 125:679–690.